

Adsorption of Methyl Orange Dye Using Fe-Mn Composite Powder as Adsorbent

Akash Deb

Department of Civil Engineering
National Institute of Technology Agartala
Agartala, India

Abstract— In this study Fe-Mn composite powder was synthesized and used as an adsorbent for the removal of Methyl Orange (MO) from aqueous solution. The effect of various parameters such as pH (2.0-8.0), contact time (2 to 30 min), adsorbent dose (0.25-1g/L) and initial concentration of dye (40-140 mg/L) on the adsorption process were studied. The optimum removal of the MO was at low pH (pH=2.0) and at with an initial concentration of 140 mg/L. CR removal of 85.93 % was achieved within 30 min. The maximum capacity of the adsorbent was found 405.11 mg/g. The experimental results were best fitted by Langmuir isotherm. Langmuir adsorption isotherm model reflects monolayer adsorption and adsorption takes place at specific homogeneous sites within the adsorbent. The adsorption kinetics was well described by pseudo-second-order reaction model. Pseudo-second-order model suggested that adsorption is chemisorptions in nature.

Keywords— Methyl Orange dye, Adsorption, Fe-Mn composite powder, Isotherm, Kinetics

I. INTRODUCTION

Dyes are widely used in industries such as the textile, pulp mill, paper, dye synthesis, food, printing, leather, and plastics industries [1, 2]. Many dyes are toxic to some organisms and can cause direct decay of aquatic living organisms. Here in this study Methyl Orange (MO, $C_{14}H_{14}N_3NaO_3S$, molecule weight 327.36 gmol/l) is selected as anionic dye model. Generally Azo dyes are well known as carcinogenic organic substances. Like many other dyes of its class, MO do not inadvertently enter the body through ingestion, it is metabolized into complex aromatic amine compounds by intestinal microorganisms [3]. Therefore, they must be removed, before discharged into natural environment, to decrease their toxic effects on environments.

There are Many different treatment methods have been developed to remove dyes from aqueous solutions, such as coagulation–flocculation, biodegradation, ion-exchange, chemical oxidation, Nano filtration and adsorption[4–7]. Among all of these methods, adsorption has been widely used for removal of dye. Adsorption method has been found to be highly efficient for the removal of color in terms of ease of operation, initial cost and simplicity of design [8]. It should be noted that, in the adsorption process, the choice of the adsorbents for treating industrial wastewater is very important factor for getting high removal.

A large variety of adsorbent materials has been proposed and investigated their ability to remove dyes such as activated carbon, natural materials, and waste materials from agricultural waste industries [9–11]. However, the adsorption capacities of the above adsorbents are not very much. In addition, due to high cost of preparation, difficult disposal and regeneration,

some of these adsorbents are difficult to be widely used. Then, to overcome the above disadvantages, magnetic nanoparticles are considered to be possible adsorbents for aqueous pollutants remaining to the high surface area and their easy separation under external magnetic fields [12].

II. MATERIALS AND METHODS

A. Chemicals and reagents

All chemical reagents Ferric chloride anhydrous ($FeCl_3$), Manganese chloride hexa-hydrate ($MnCl_2 \cdot 6H_2O$), and MO solution were used as a model synthetic contaminant. Nano pure water was used throughout the experiment. The chemicals used in this study were mostly of higher reagent grades.

B. Synthesis and characterization of adsorbent

Fe-Mn magnetic adsorbent was synthesized using co-precipitation method. In this synthesis, two separate homogeneous solutions of $FeCl_3$ and $MnCl_2 \cdot 6H_2O$ were prepared dissolving 27.1 g of $FeCl_3$ and 15.73 $MnCl_2 \cdot 6H_2O$ each in two separate beakers containing 250mL of DI water, respectively. Another homogeneous solution of NaOH was prepared by dissolving 40.0 g of NaOH pellet in 500mL DI water at room temperature. The ratio of Fe-Mn was 2:1. Both the solutions of $FeCl_3$ and $MnCl_2 \cdot 6H_2O$ were then added to the NaOH solution slowly and stirring was continued till the formation of a brownish precipitate. The resulting precipitates were filtered and dried in air at 110°C overnight. Afterward the solid samples were then washed with DI water to remove any traces of chlorine, excess alkali, or other impurities. Then, the washed solid was calcined at 400°C under air for 8 hours. The adsorbent was cooled at room temperature and crushed to get a fine powder. These fine powders were used in the adsorption experiment.

C. Batch mode adsorption studies

The adsorption of MO onto Fe-Mn composite powder was studied by a batch method. A certain amount of adsorbent was placed in a 250 mL flask, into which desired concentration MO solution was added. The adsorption experiments were performed in a room temperature. The supernatant was measured using a UV–vis spectrometer at 464 nm for its residual MO concentration. The different parameters studied included: (i) effect of pH: (2.0–8.0) (ii) effect of different initial MO concentrations (40, 60, 80, 100, 120 and 140 mg/L); at a room temperature, (iii) effect of adsorbent dosage: (0.25–1.0 g/L) and (iv) effect of contact time: (2–30 min) at a constant temperature. The solution was stirred for different

time intervals and then allowed to settle down and were removed using magnetic filtration.

Besides, the adsorption isotherms at different temperatures and pH values of MO solutions were investigated to understand the adsorption behavior. And the kinetics was also evaluated at different concentrations and pH values of MO solutions to investigate the adsorption characteristic.

The amount of CR adsorbed per unit mass of the adsorbent (q_e , mg/g) was calculated using the following equation:

III. RESULT AND DISCUSSIONS

A. Effect of pH

The pH value of MO solution plays an important role in the whole adsorption process, influencing not only the surface charge of the adsorbent, and the dissociation of functional groups on the active sites of the adsorbent, but also the chemistry of MO solution. The effect of pH value of initial MO solutions on adsorption is shown in Fig. 2b. The removal efficiency increased from 34.26% to 89.47% when the pH was changed from 8.0 to 2.0 and maximum adsorption was observed at pH 2.0. MO is an anionic acid dye because of the presence of negative sulfonate ion (SO_3^-) in its structure. In acidic medium, the lower pH leads to an increase in H^+ ion concentration and the adsorbents surface becomes more positively charged. The strong electrostatic attraction between the positively charged adsorption site and the anionic MO molecule results in high adsorption of MO dye[13]. Furthermore, the higher adsorption capacity may be attributed to more hydrogen bonding formed from $-\text{SO}_3^-$ to $-\text{SO}_3\text{H}$ at lower pH. At higher pH values the adsorbent surface gets negatively charged due to OH^- ions which results in the decrease of MO percentage removal due to electrostatic repulsion. pH 2.0 is chosen throughout this study for analysis of other parameters and also for equilibrium and kinetic studies[14,15,16].

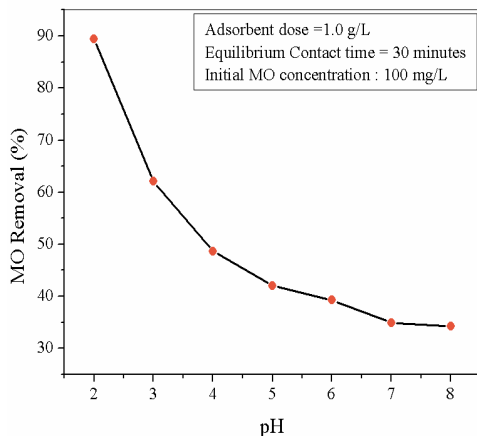


Fig.2. Effect of pH on the adsorption of MO

B. Effect of Initial CR concentration

Effect of initial concentrations of MO on the adsorption capacity of Fe-Mn composite powder had been studied for different initial concentrations of 40 to 140 mg/L through batch experiment mode at pH of 2.0, contact time of 2 to 30 minutes and with a fixed adsorbent dose of 1g/L as shown in figure 3. As seen in Fig. 3, adsorption capacity value enhances evidently from 21.902 mg.g⁻¹ to 114.75 mg.g⁻¹ with the increase in the initial concentration from 40mg/L to 140 mg/L. The increase in capacity could be due to the increase in the electrostatic

interactions between the dye molecules and the adsorbent. The actual amount of dye adsorbed per unit mass of adsorbent increased with increase in dye concentration, this increase in capacity may be also due to the presence of effective binding sites [17, 18].

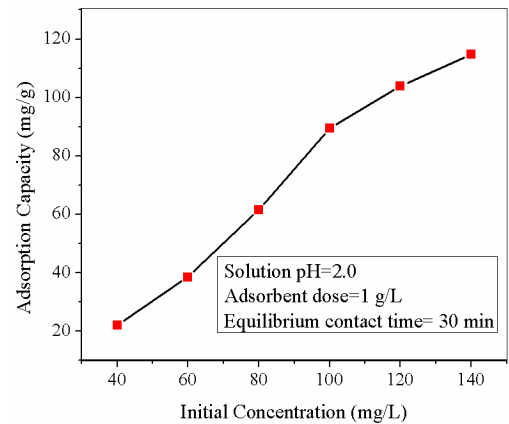


Fig.3. Effect of initial concentration on the adsorption of MO

C. Effect of Adsorbent dose

In order to investigate the effect of adsorbent mass on the adsorption, a series of adsorption experiments was carried out with different adsorbent dosages at initial concentration of 140 mg/L without changing the volume of dye solution (50 ml) at pH of 2.0. It is seen that the adsorption capacity decreases with increasing adsorbent dose irrespective of the dye concentration. Such performance on the adsorbent may be due to the fact that some of the adsorption sites remain unsaturated during the adsorption process. This decrease in adsorption capacity may be due to overlapping or aggregation of adsorption sites resulting in a decrease in total adsorbent surface area available to the dye for adsorption.

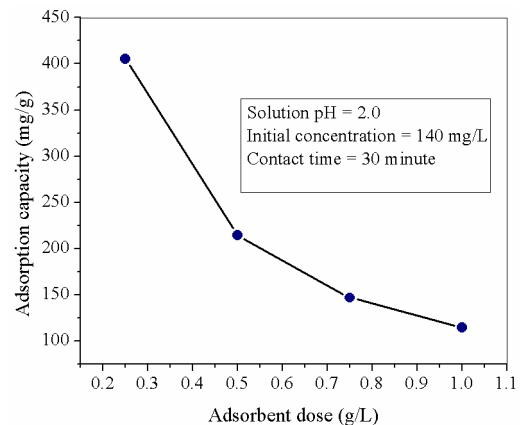


Fig. 4. Effect of adsorbent dose on the adsorption of MO

D. Effect of time

The effect of time on the removal efficiency of the MO were also studied at fixed adsorbent dose 1 g/L, pH of 2.0, and 100 mg/L for different time intervals and the results are shown graphically in Figure 5. It had been established that optimum time required to attain the equilibrium between the MO adsorbed on bi metal oxide particles was within 30 min. At this time the adsorption efficiency of 100mg/L MO concentration was observed to be 89.47 %.

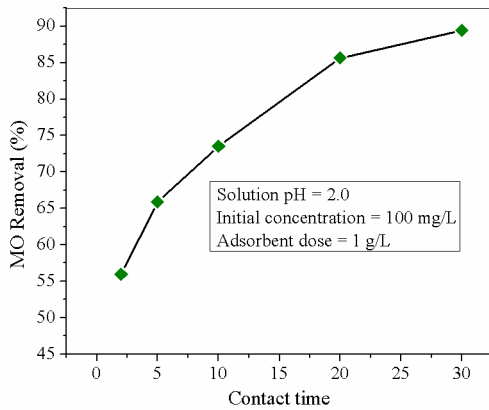


Fig.5. Effect of contact time on the adsorption of MO

E. Kinetic modeling

Kinetic performance of a given adsorbent is of utmost important to get an indication about the solute uptake rate. Contact time plays an important role in affecting efficiency of adsorption. In order to optimize the contact times for the maximum uptake of adsorbate Pseudo first order and second order kinetics model were analysed for mechanism of MO adsorption.

Lagergren-first-order kinetic model might be represented by [19]:

$$\log(q_{1e} - q_t) = \log q_{1e} - \frac{K_1 t}{2.303} \quad (2)$$

A linear form of pseudo-second-order kinetic model was expressed by [20]:

$$\frac{t}{q_t} = \frac{1}{K_2 \times q_{2e}^2} + \frac{t}{q_{2e}} \quad (3)$$

Where q_{1e} and q_{2e} are the amounts of adsorbate adsorbed (mg/g) at equilibrium, q_t is the amount of adsorbate adsorbed at time t (min) respectively; k_1 is the rate constant of Lagergren-first-order kinetic model (min^{-1}); k_2 ($\text{g mg}^{-1} \text{min}^{-1}$) is the rate constant of pseudo second order adsorption.

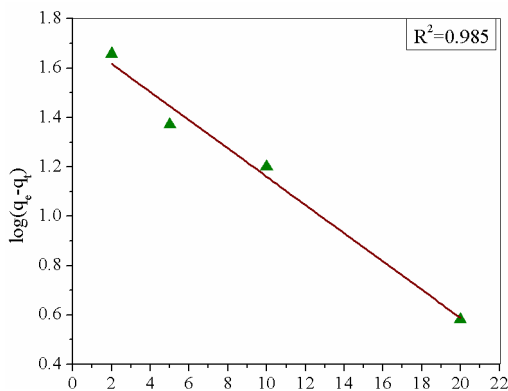


Fig.6. Pseudo-first order kinetic model

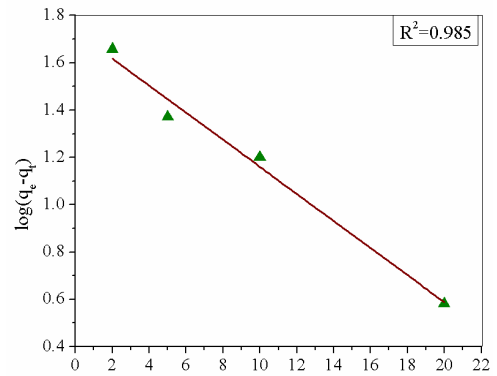


Fig.7. Pseudo-second order kinetic model

A Table.1. Kinetic parameters for MO removal with adsorbent dosage of 1.0 g/L over initial concentrations 100–140 mg/L

Model	Parameters	CR Concentration		
		100 mg/L	120 mg/L	140 mg/L
Pseudo first order	K_1	0.131	0.117	0.088
	q_{1e} (calc.)	53.951	27.797	25.293
	R^2	0.985	0.790	0.847
Pseudo second order	K_2	0.004	0.009	0.009
	q_{2e} (calc.)	100	111.111	125
	R^2	0.999	0.999	0.999
Experimental data	q_e (exp.)	89.472	103.916	114.75

The parameters as obtained from the plots are given in Table 1. As observed, the calculated adsorption capacity $q_e(\text{cal})$ for pseudo-second-order model was much more closer to the experimental adsorption capacity $q_e(\text{exp})$ for various MO concentrations confirming better applicability of pseudo second-order model compared to pseudo-first-order model. These results are further confirmed by higher regression coefficient (R^2) values for pseudo-second-order model compared to pseudo-first order model. Thus, it indicates that the adsorption of MO on metal oxide particles is a chemisorption process [21].

F. Isotherm modeling

The analysis of the isotherm data is important for developing equations, which will accurately represent the results and could be used for designing process.

In this study, the equilibrium adsorption of MO was investigated at adsorbent doses 1.0 g/L and optimum values of other variables. The Langmuir and Freundlich isotherm models were applied to the adsorption data obtained from batch studies and shown in Fig.8 and 9 respectively. Langmuir adsorption isotherm model assumes monolayer adsorption and adsorption takes place at specific homogeneous sites within the adsorbent. All the sites are considered as identical and energetically equivalent, once adsorbate molecule occupies a site, no further adsorption can take place in the same site.

The Langmuir equation can be expressed as follows [22]:

$$\frac{C_e}{q_e} = \frac{Q_m}{K_a} + \frac{C_e}{Q_m} \quad (4)$$

Where, q_e is the amount of adsorbate adsorbed at the time of equilibrium in mg/g, C_e is the equilibrium concentration of adsorbate in the solution in mg/L, Q_m is the maximum adsorption capacity in mg/g and K_a is the Langmuir isotherm constant in L/mg.

Applicability of the Langmuir isotherm can be found out by determining a dimensionless separation factor (R_L) and error analysis by following equation:

$$R_L = \frac{1}{1 + K_a \times C_0} \quad (5)$$

C_0 (mg/L) is the initial adsorbate concentration in the solution. The value of R_L gives insight into the suitability of adsorbent for the adsorption i.e., affinity between adsorbate and adsorbent (Montoya et al. 2013). If, $R_L < 1.0$ it represents favorable adsorption; $R_L > 1.0$ it represents unfavorable adsorption; and $R_L = 0$ irreversible adsorption.

Freundlich isotherm model reflects the multilayer adsorption and applicable for heterogeneous adsorption surfaces. This model can be represented by below equations [23]:

$$\ln q_e = \ln K_f + 1/n \ln C_e \quad (6)$$

Where q_e is the amount of adsorbate at equilibrium time in mg/g, C_e is the equilibrium concentration of adsorbate in the solution in mg/L, K_f is the capacity of the adsorbent in mg/g and n is the adsorption constant for Freundlich isotherm in L/mg, usually greater than one. It can be stated that, if the $1/n$ value is below unity, this implies that the adsorption process is chemical and if the value is above unity, adsorption is a favourable physical process.

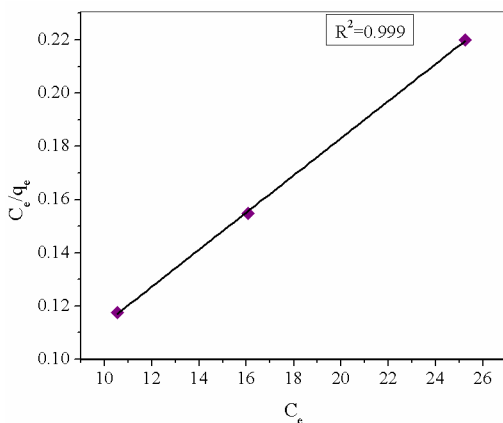


Fig.8. Langmuir isotherm model fitting for MO adsorption

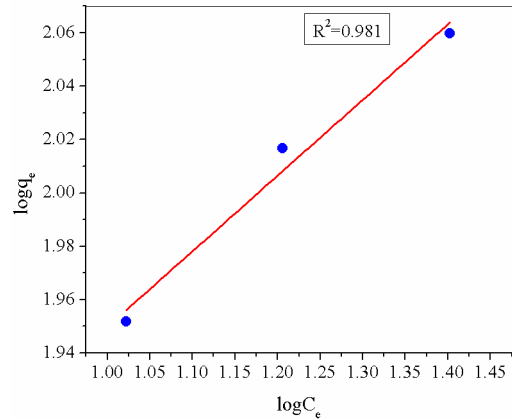


Fig.9. Freundlich isotherm model fitting for MO adsorption

The isotherm parameters were calculated and presented in Table 2

Table.2. Comparison between different isotherm parameters

Isotherm	Parameters	Adsorbent Dose	
		0.5 g/L	1.0 g/L
Langmuir isotherm	Q_m (mg/g)	333.333	90.909
	K_a	10752.688	3322.2558
	R_L	1.075269×10^{-5}	3.322256×10^{-5}
	R^2	0.999	0.999
Freundlich isotherm	K_f (mg/g)	79.983	46.345
	n	3.521	3.534
	R^2	0.989	0.981

Based on the linear form of Freundlich isotherm model, the K_f and n values were obtained from the intercept and the slope of the $\ln C_e$ vs. $\ln q_e$ plot respectively. In case of Langmuir isotherm K_a and Q_m values are determined from the intercept and slope of C_e vs. (C_e / q_e) plot. The high R^2 value for Langmuir isotherm shows that the mechanism of adsorption follows Langmuir isotherm. Thus between the two isotherms Langmuir isotherm was the most suitable and provides best correlation for the experiment results.

G. Comparison with other adsorbents

From the published literature, other CR removal adsorption techniques were studied and their performance in terms of adsorption capacity were compared and listed in Table 3

Table.3. Comparison between the present study and other adsorbents in terms of adsorption capacity

Adsorbent	Adsorption capacity (mg/g)	Reference
Banana peel	21	24
Orange peel	20.5	24
Hyper cross linked polymeric adsorbent	70.9	25
Fe-Mn bi metal oxide	405.111	In this paper

IV. CONCLUSION

The Fe-Mn composite powder has been synthesized using precipitation method. Batch experiments were performed for the removal of MO dye from aqueous solution, using bi metal oxide as adsorbent materials. Adsorption study was carried out by changing different parameters such as effect of time, pH and solution concentrations. MO removal efficiency is strongly affected by pH of reaction mixture, with increasing pH, decreasing in percentage removal. It is found that the adsorption capacity increases with increasing initial concentration but the capacity was decreased with increasing adsorbent dose. The maximum removal was get at acidic pH Adsorption equilibrium is attained within a contact time of 30 min. The adsorption capacity was found to be 405.111 mg/g approximately. The order of MO adsorption was governed by pseudo-second-order kinetics. Pseudo-second-order model suggested that adsorption is chemisorptions in nature. the mixed composite material obeyed Langmuir isotherm model as compared to Freundlich isotherm.

REFERENCES.

- [1] Yagub M. T., Sen T. K., Afroze S., & Ang H. M. (2014). Dye and its removal from aqueous solution by adsorption: a review. *Advances in colloid and interface science*, 209, pp: 172-184.
- [2] Wang T., Kailasam K., Xiao P., Chen G., Chen L., Wang L., ... & Zhu J. (2014). Adsorption removal of organic dyes on covalent triazine framework (CTF). *Microporous and Mesoporous Materials*, pp: 187, 63-70.
- [3] Mittal A., Malviya A., Kaur D., Mittal J., & Kurup L. (2007). Studies on the adsorption kinetics and isotherms for the removal and recovery of Methyl Orange from wastewaters using waste materials. *Journal of Hazardous Materials*, pp:148(1), 229-240.
- [4] Doğan M., Abak H., & Alkan M. (2008). Biosorption of methylene blue from aqueous solutions by hazelnut shells: equilibrium, parameters and isotherms. *Water, air, and soil pollution*, 192(1-4), pp:141-153.
- [5] Ghaedi M., Hassanzadeh A., & Kokhdan S. N. (2011). Multiwalled carbon nanotubes as adsorbents for the kinetic and equilibrium study of the removal of alizarin red S and morin. *Journal of Chemical & Engineering Data*, 56(5), pp: 2511-2520.
- [6] Chatterjee, S., Lee, M. W., & Woo, S. H. (2010). Adsorption of congo red by chitosan hydrogel beads impregnated with carbon nanotubes. *Bioresource Technology*, 101(6), pp: 1800-1806.
- [7] Wang L., & Wang A. Q. (2007). Removal of Congo red from aqueous solution using a chitosan/organo-montmorillonite nanocomposite. *Journal of Chemical Technology and Biotechnology*, 82(8), pp: 711-720.
- [8] Garg V. K., Kumar R., & Gupta R. (2004). Removal of malachite green dye from aqueous solution by adsorption using agro-industry waste: a case study of *Prosopis cineraria*. *Dyes and Pigments*, 62(1), pp: 1-10.
- [9] Shao L., Ren Z., Zhang G., & Chen L. (2012). Facile synthesis, characterization of a MnFe_2O_4 activated carbon magnetic composite and its effectiveness in tetracycline removal. *Materials Chemistry and Physics*, 135(1), pp:16-24.
- [10] Yang N., Zhu S., Zhang D., & Xu S. (2008). Synthesis and properties of magnetic Fe_3O_4 -activated carbon nanocomposite particles for dye removal. *Materials Letters*, 62(4), pp: 645-647.
- [11] Ozdemir O., Armagan B., Turan M., & Celik M. S. (2004). Comparison of the adsorption characteristics of azo-reactive dyes on mesoporous minerals. *Dyes and Pigments*, 62(1), pp: 49-60.
- [12] Iram M., Guo C., Guan Y., Ishfaq A., & Liu H. (2010). Adsorption and magnetic removal of neutral red dye from aqueous solution using Fe_3O_4 hollow nanospheres. *Journal of hazardous materials*, 181(1), pp: 1039-1050.
- [13] Dutta A., & Dutta R. K. (2014). Fluorescence behavior of cis-methyl orange stabilized in cationic premicelles. *Spectrochimica Acta Part A: Molecular and Biomolecular Spectroscopy*, 126, pp: 270-279.
- [14] Zhang R., Zhang J., Zhang X., Dou C., & Han R. (2014). Adsorption of Congo red from aqueous solutions using cationic surfactant modified wheat straw in batch mode: Kinetic and equilibrium study. *Journal of the Taiwan Institute of Chemical Engineers*, 45(5), pp: 2578-2583.
- [15] Tabak A., Baltas N., Afsin B., Emirik M., Caglar B., & Eren E. (2010). Adsorption of Reactive Red 120 from aqueous solutions by cetylpyridinium-bentonite. *Journal of chemical technology and biotechnology*, 85(9), pp: 1199-1207.
- [16] Foroughi-dahr M., Abolghasemi H., Esmaili M., Nazari G., & Rasem B. (2015). Experimental study on the adsorptive behavior of Congo red in cationic surfactant-modified tea waste. *Process Safety and Environmental Protection*, 95, pp: 226-236.
- [17] Yao Y., Bing H., Feifei X., & Xiaofeng C. (2011). Equilibrium and kinetic studies of methyl orange adsorption on multiwalled carbon nanotubes. *Chemical Engineering Journal*, 170(1), pp: 82-89.
- [18] Wu F. C., Tseng R. L., & Juang R. S. (2001). Kinetic modeling of liquid-phase adsorption of reactive dyes and metal ions on chitosan. *Water Research*, 35(3), pp: 613-618.
- [19] Zhu H. Y., Jiang R., Xiao L., & Zeng G. M. (2010). Preparation, characterization, adsorption kinetics and thermodynamics of novel magnetic chitosan enwrapping nanosized $\gamma\text{-Fe}_2\text{O}_3$ and multi-walled carbon nanotubes with enhanced adsorption properties for methyl orange. *Bioresource technology*, 101(14), pp: 5063-5069.
- [20] Wu C. H. (2007). Adsorption of reactive dye onto carbon nanotubes: equilibrium, kinetics and thermodynamics. *Journal of Hazardous materials*, 144(1), pp: 93-100.
- [21] Chiou M. S., Ho P. Y., & Li H. Y. (2004). Adsorption of anionic dyes in acid solutions using chemically cross-linked chitosan beads. *Dyes and Pigments*, 60(1), pp: 69-84.
- [22] Ai L., & Jiang J. (2010). Fast removal of organic dyes from aqueous solutions by AC/ferrospinel composite. *Desalination*, 262(1), pp: 134-140.
- [23] Vimonses V., Lei S., Jin B., Chow C. W., & Saint C. (2009). Adsorption of congo red by three Australian kaolins. *Applied Clay Science*, 43(3), pp:465-472
- [24] Annadurai G., Juang R. S., & Lee D. J. (2002). Use of cellulose-based wastes for adsorption of dyes from aqueous solutions. *Journal of hazardous materials*, 92(3), pp: 263-274.
- [25] Huang J. H., Huang K. L., Liu S. Q., Wang A. T., & Yan C. (2008). Adsorption of Rhodamine B and methyl orange on a hypercrosslinked polymeric adsorbent in aqueous solution. *Colloids and Surfaces A: Physicochemical and Engineering Aspects*, 330(1), pp: 55-61.